# Comparison of field and laboratory collected midwave and longwave infrared emissivity spectra / data reduction techniques

Carl Salvaggio*, Craig J. Miller**
Spectral Information Technology Applications Center

## ABSTRACT

Many targets that remote sensing scientists encounter when conducting their research experiments do not lend themselves to laboratory measurement of their surface optical properties. Removal of these targets from the field can change their biotic condition, disturb the surface composition, and change the moisture content of the sample. These parameters, as well as numerous others, have a marked influence on surface optical properties such as spectral and bi-directional emissivity. This necessitates the collection of emissivity spectra in the field. The propagation of numerous devices for the measurement of midwave and longwave emissivity in the field has occurred in recent years. How good a re these devices and how does the accuracy of the spectra they produce compare to the "tried and true" laboratory devices that have been around for decades? A number of temperature/emissivity separation algorithms will be demonstrated on data collected with a field portable Fourier transform infrared (FTIR) spectrometer and the merits and resulting accuracy compared to laboratory spectra made of these identical samples. A brief look at off-nadir view geometries will also be presented to alert scientists to the possible sources of error in these spectra that may result when using sensing systems that do not look straight down on targets or when their nadir looking sensor is looking at a tilted target.

Keywords: longwave, midwave, emissivity, ground truth, laboratory, spectra, spectroscopy, hyperspectral

## 1. INTRODUCTION

The field of hyperspectral remote sensing and the exploitation of this data rely heavily on an analyst or scientist's understanding of the phenomenology present on the ground. Knowledge of the reflectance and emissivity spectra for targets that are under study is important both in planning and subsequent study of this data. It is important to understand, however, that the knowledge of a material's optical properties is not only limited to a measurement made in the laboratory. The way a material interacts with its background and the environment in which it exists is what is recorded by a remote sensing platform and therefore is ultimately what needs to be understood. Laboratory measurements may provide the scientist with initial data that can be used to determine feasibility of detection or identification of materials, but it is the measurement of these properties in the field that will ultimately determine the performance of an algorithm under real world conditions.

While laboratory measurements have been made for many decades in the midwave (MWIR) and longwave (LWIR) infrared portions of the spectrum, field measurements do not have such a legacy. The measurement of radiance and derivation of emissivity in the field have many obstacles to overcome and rely heavily on the scientist's understanding of the phenomenology they are measuring. It is the purpose of this paper to describe efforts that have taken place to assure us that our methods in the field provide data that is of equal quality to that obtained in the laboratory. Where this is not the case, it is equal if not more important to understand why it is not and what we can expect from real-world sensing systems.

## 2. BACKGROUND

The radiance field that you observe with a sensor is a function of many contributing parameters. These parameters include the material's optical properties, source and background radiance, and the intervening atmosphere. If all of the atmospheric, source and background effects can be accounted for (or their effects minimized) then the radiance you are left with is the radiance leaving a surface due to its self-emission. This self-emission term is complicated by the fact that it is a function of two parameters, the spectral diffuse hemispheric emissivity and the surface temperature of the target, $\varepsilon(\theta_t,\lambda)$ and $T_s$, respectively. This self-emission term $L_s(\theta_t,T_s,\lambda)$ is given by

$$L_S(\theta_t, T_S, \lambda) = \varepsilon(\theta_t, \lambda) L_{BB}(T_S, \lambda) \tag{1}$$

*carl@imagerysolutions.com; 1 703 591-8546 ext. 200; fax 1 703 591-2437; Spectral Information Technology Applications Center, 11781 Lee Jackson Memorial Highway, Suite 400, Fairfax, VA 22033-3309; **cjm@photon.com; 1 703 591-8546 ext. 170; fax 1 703 591-2437; Spectral Information Technology Applications Center, 11781 Lee Jackson Memorial Highway, Suite 400, Fairfax, VA 22033-3309

Algorithms for Multispectral, Hyperspectral, and Ultraspectral Imagery VII, Sylvia S. Shen, Michael R. Descour, Editors, Proceedings of SPIE Vol. 4381 (2001)

and, where the spectral emissivity for a material is defined as

$$\varepsilon(\theta_t,\lambda) = \frac{L_s(\theta_t, T_s, \lambda)}{L_{BB}(T_s,\lambda)} \tag{2}$$

In practice, this self-emission term cannot be measured directly, but the atmospheric effects can be minimized by taking measurements close to the material surface. If this is done then the transmission of the path from the material to the sensor approaches unity and the emitted and scattered path radiance is negligible. At this point, the radiance that is measured is the self-emission and reflected background. Making these atmospheric minimizing assumptions, the total sample leaving radiance is stated as

$$L(h,\theta,\lambda) = \varepsilon(\theta_t,\lambda)L_{BB}(T_s,\lambda) + (1-\varepsilon(\theta_t,\lambda))L_{DWR}(\lambda) \tag{3}$$

where $L_{DWR}(\lambda)$ is the total spectral downwelling radiance from the hemisphere above the material. Solving Equation 3 for the target spectral emissivity yields

$$\varepsilon(\theta_t,\lambda) = \frac{L(h,\theta,\lambda) - L_{DWR}(\lambda)}{L_{BB}(T_s,\lambda) - L_{DWR}(\lambda)} \tag{4}$$

This result allows one to compute the spectral emissivity of a sample from the measurement of surface leaving and downwelling radiance, as well as the material's surface temperature, $T_s$. The surface temperature may or may not be known at the time radiance measurements are made. Some materials are not readily amenable to surface temperature measurement (e.g. vegetation). If a direct measurement of $T_s$ can be made then the spectral emissivity can be calculated directly. If a direct measure of surface temperature is unavailable, there are a number of methodologies in varying stages of development for deriving spectral emissivity. Several of these will be compared in the following analysis along with the comparison of field and laboratory spectra. The Designs and Prototypes Model 102 Field Spectrometer[1,2] used to measure radiance for this study contains a simple, yet relatively effective, temperature-emissivity separation algorithm. Several others that have been described in the literature have been implemented in an IDL program designed to utilize the radiance spectra directly from the field spectrometer. A brief summary of the temperature-emissivity separation problem and the techniques implemented and used in this study follows.

The problem that exists in determining spectral emissivity from the measurement of radiance is that the simultaneous solution for sample temperature and spectral emissivity is always underdetermined for a spectral radiance measurement. There is always one more unknown than there are equations. For an $n$-channel spectral radiance measurement, one records $n$ values for $L(h,\theta,\lambda)$, however, there are $n$+1 unknowns, the $n$-values of $\varepsilon(\theta_t,\lambda)$ and $T_s$.

Reference Channel (REFCHAN)

One of the simplest techniques for determining these parameters is presented by Kahle and Alley[3] and has been suggested by many other researchers prior to this. The technique is denoted as the maximum emissivity or reference channel method. An assumption is made that at some wavelength within the spectral region of concern, the sample being measured has a spectral emissivity value equal to unity. Given this assumption of unit emissivity at a particular wavelength, $\lambda_0$, Equation 3 can be rearranged, inverted and solved for temperature, $T_s$, at this wavelength.

$$L_{BB}(T_s,\lambda_0) = \frac{L(h,\theta,\lambda_0) - (1-\varepsilon(\theta_t,\lambda_0))L_{DWR}(\lambda_0)}{\varepsilon(\theta_t,\lambda_0)}$$

$$T_s = \frac{\dfrac{4387.9}{\lambda_0}}{\ln\left\{\left(\dfrac{3.7418x10^8}{\lambda^5}\dfrac{L(h,\theta,\lambda_0) - (1-\varepsilon(\theta_t,\lambda_0))L_{DWR}(\lambda_0)}{\varepsilon(\theta_t,\lambda_0)}\right)+1\right\}} \tag{5}$$

Under the assumption that $\varepsilon(\theta_t,\lambda_0)$=1, this reduces to

$$T_s = \frac{4387.9}{\lambda_0} \frac{1}{\ln\left\{\left(\frac{3.7418x10^8}{\lambda^5 L(h,\theta,\lambda_0)}\right)+1\right\}} \tag{6}$$

This temperature can then be used to solve for the spectral emissivity at all *n*-1 other wavelengths using Equation 4 and the measured spectral radiance.

The assumptions in this method are quite restrictive and this technique must be used with a cognizance of its limitations. More often than not, the sample being measured will not have a wavelength within its spectrum where the emissivity is unity. This is certainly the case for most man-made materials. Assuming unit emissivity in these cases will upwardly bias the magnitude of the entire spectrum. A modification to this technique is often proposed which allows for a maximum, non-unit, emissivity to be specified at a particular wavelength, $\lambda_0$. While making the technique a bit less restrictive, it still suffers from another limitation of the maximum emissivity method, the requirement for *a priori* knowledge of the sample's maximum emissivity and the wavelength at which it occurs. Given that laboratory measurements are made for the material, this is not inconceivable data to expect, however, many field-measured samples do not lend themselves to laboratory measurements for physical or biophysical reasons. This makes the assumed data difficult to come by.

Blackbody Fit (BBFIT)

A second similar method referred to as the blackbody fit method searches for the blackbody radiance curve that results in an emissivity spectra that peaks at a specified maximum emissivity within a user defined wavelength interval. Two arbitrary temperature values are chosen to bracket the actual surface temperature of the sample measured. The temperature range is bisected and the central temperature used to compute a current estimate for the spectral blackbody radiance. This radiance curve is then used to compute the current estimate of spectral emissivity of the sample using Equation 4 and the measured downwelling radiance. The maximum value of the emissivity curve in the user specified wavelength range is then compared to the user specified maximum value for this range. If the current estimate is greater than the specified maximum value, the upper end of the temperature range is decreased to match the current temperature and the process repeated. If the current maximum emissivity estimate was less than specified value, the lower end of the range would be increased to the current temperature before repeating. The process is continued until the temperature range collapses to a predefined limit (*e.g.* the range was collapsed to a limit of 0.0001°C for this study).

As with the maximum emissivity method, the limitations of this method include knowing an emissivity for the sample in a particular wavelength region. In this case, it may be less restrictive since you can choose the range in a region where the sample acts like a blackbody. If this is not known a priori, one can look at the acquired radiance spectra and determine a region in which there is little or no structure in the spectra. This would be a suitable region to choose with a maximum emissivity set to unity. For the materials used in this study, the region from 7.5 to 8 μm always served as a good fitting region.

Maximum Spectral Temperature (MAXSPEC)

Relaxing the assumptions of the maximum emissivity and blackbody fit methods, Korb *et al.*[4] have developed a technique, referred to as the maximum spectral temperature method, that only requires *a priori* knowledge of the wavelength at which the maximum emissivity, $\varepsilon_{max}$, occurs, not its magnitude. Salisbury and D'Aria[5,6] have published these peak emissivity wavelength values for a large number of naturally occurring materials in both the 3 to 5 μm and 8 to 14 μm wavelength regions. Assuming $\varepsilon_{max}$ is constant for all wavelengths, spectrally flat, the spectral self-emitted radiance is equivalent to a blackbody emission at the surface temperature provided that the fractional downwelling radiance is subtracted and the remaining self-emitted radiance is scaled by the maximum emissivity.

$$L_{BB,\max}(\lambda,T_s) = \frac{L(h,\theta,\lambda) - L_{DWR}(\lambda)}{\varepsilon_{\max}} + L_{DWR}(\lambda) \tag{7}$$

Inverting this to solve for temperature, one obtains a "spectral temperature" curve as

$$T_s(\lambda) = \frac{4387.9}{\lambda} \frac{1}{\ln\left\{\left(\frac{3.7418x10^8}{\lambda^5 L_{BB,\max}(\lambda, T_s)}\right) + 1\right\}} \tag{8}$$

When $T_s(\lambda)$ is plotted as a function of wavelength, $T_s(\lambda)$ is only correct where $\varepsilon(\lambda)=\varepsilon_{max}$. At all other wavelength values, $T_s(\lambda)$ is too low, *i.e.* the best estimate of the surface temperature is the highest temperature in the spectrum for a noise free measurement. Since all measurements contain noise, this spectrum is smoothed to average out noise that may exist and the maximum temperature determined. The spectral emissivity is then computed using Equation 2 with the maximum average temperature. The same smoothing function is applied and the emissivity computed is compared to the $\varepsilon_{max}$ with which you started. If these values are different, then the temperature is incremented by a small amount and the spectral emissivity recomputed. This is carried out until these emissivities match within a specified tolerance, usually 0.001.

Spectral Smoothness (SMOOTHNESS)

An even less restrictive technique that has been employed by both Horton *et al.*[7] and Bower *et al.*[8] referred to as the spectral smoothness method does not require a knowledge of the maximum emissivity or the wavelength at which it occurs. In a similar development to that already shown, these teams derive absolute spectral emissivity as shown in Equation 4.

The measurement of downwelling radiance typically involves measuring the radiance from an InfraGold reflectance standard in the same configuration as the sample material. The radiance leaving the InfraGold plate in the absence of an intervening atmosphere is composed of two terms, the reflected downwelling and self-emitted radiance given as

$$L_G(\lambda) = \varepsilon_G(\lambda) L_{BB}(T_G, \lambda) + (1 - \varepsilon_G(\lambda)) L_{DWR}(\lambda) \tag{9}$$

where $L_G(\lambda)$ is the measured spectral radiance from the diffuse gold plate, $\varepsilon_G(\lambda)$ is the spectral emissivity of the diffuse gold plate, and $T_G$ is the temperature of the diffuse gold plate. Solving for the downwelling radiance yields

$$L_{DWR}(\lambda) = \frac{L_G(\lambda) - \varepsilon_G(\lambda) L_{BB}(T_G, \lambda)}{1 - \varepsilon_G(\lambda)} \tag{10}$$

The premise of this technique is that for measurements made over a very short sample to sensor path, the atmospheric transmission is unity and the intervening path radiance is negligible (the same assumption made in the derivation of Equation 3). This leaves only three parameters necessary to derive spectral emissivity for the target; the spectral emissivity of the gold plate, the temperature of the gold plate during the downwelling radiance measurement, and the target's surface temperature during its measurement. Horton, *et al.*[7] have shown for their measurements that reasonable errors in specifying the emissivity of the gold plate as well as for it's temperature have relatively small effects on the computation of spectral emissivity. The effects of a 50% to 200% error in specifying the scalar gold plate emissivity resulted in errors of approximately 0.02 to 0.04 for the target spectral emissivity in the reststrahlen bands. Far smaller errors were observed in all other portions of the 8 to 13 μm window in which they were working. They also showed that due to the low emissivity of the diffuse gold plate, the effect of significant errors in the gold plate temperature had little effect on the resulting target spectral emissivity curve. Errors of +12°C and –8°C were introduced which produced little variance in the final emissivity curves derived. The only parameter that produced a significant error over the entire spectrum was the target's surface temperature.

Two effects were noted when the target temperature was incorrectly estimated. The first was that the entire calculated target emissivity spectrum was affected, not only in the reststrahlen bands. The second was that the atmospheric emission lines were accentuated in either the positive or negative direction by a poor estimate of the target temperature. If the target temperature was underestimated the atmospheric emission lines remained in the derived emissivity spectrum, especially in the reststrahlen bands. If the target temperature is overestimated, underestimates of target spectral emissivity are obtained and atmospheric emission lines are reintroduced to the spectrum in an opposite sense.

Horton *et al.*[7] have proposed a method that arrives at the target surface temperature by minimization of the reflected atmospheric emission lines within a portion of the measured spectrum. They used the portion of the spectrum around the short wavelength lobe of the silicate doublet, 8.12 to 8.60 μm, in the reststrahlen bands. Holding the temperature and scalar emissivity of the gold plate constant, they varied the temperature of the target in 0.5°C increments around the postulated target surface temperature. They fit a second order polynomial through the derived emissivity spectrum within the region mentioned above. Residual errors are computed between the derived target emissivity spectra and the computed second-order polynomial. These residuals are plotted as a function of temperature. The target temperature is determined to be that temperature at which this residual curve goes though a minimum. While originally intended to be a methodology for

determining absolute spectral emissivity, for which it proves to be a good technique, this procedure also serves as a target temperature derivation tool. The relative insensitivity of the technique to gold plate temperature and emissivity and the derivation of target temperature from measured spectral data ideally lend this technique to field work.

## 3. TECHNICAL APPROACH

The approach taken in this study to compare laboratory and field emissivity spectra was straightforward. Twelve materials samples including fabrics, building materials, films and naturally occurring substances were chosen and measurements made in the laboratory and the field under "ideal" conditions. Laboratory measurements were made at the Air Force Research Laboratory (AFRL) facility at Wright-Patterson Air Force Base. The materials were then measured outdoors at the Spectral Information Technology Applications Center (SITAC) facility in Fairfax, Virginia. A day was chosen that had no visible cloud cover, moderate ambient temperature, low humidity and calm winds. These conditions are as ideal as possible to make outdoor field radiance measurements.

The radiance data collected in the field consisted of 4 measurements per sample. For each sample, a cold and a warm blackbody were measured for calibration purposes. The cold blackbody was set to a temperature just below the sample's temperature while the warm blackbody was set approximately 10°C above the sample temperature. These measurements were made immediately prior to measuring the sample leaving radiance to minimize the effects of instrument drift. Immediately following the measurement of the sample leaving radiance, an InfraGold reflectance standard was placed on top of the sample in an identical orientation. The radiance leaving this surface was then measured. The InfraGold reflectance standard exhibits a flat spectral reflectance across the 3 to 15 μm window with a magnitude of approximately 0.95. Taken at close range, the recorded radiance field consists of reflected downwelling radiance and self-emitted energy. The InfraGold surface temperature was also recorded and used to remove the self-emitted portion of the radiance field during the calibration process using Equation 10. The calibrated sample leaving and downwelling radiance measurements were then used to derive emissivity using the previously described methods.

## 4. RESULTS

The MWIR/LWIR spectra for a number of materials measured at the AFRL laboratory and by SITAC personnel with the Designs & Prototypes Model 102 Portable Field Spectrometer were compared. The purpose of this comparison was to validate collection methodologies and identify improvements that could be made to assure that accurate field spectra are collected. In the comparison of laboratory spectra to field spectra, the field data was reduced to emissivity using the temperature/emissivity separation algorithms described previously in this paper. Throughout this section the four methods previously described are referenced as blackbody fit (BBFIT), reference channel (REFCHAN), maximum spectral temperature (MAXSPEC) and spectral smoothness (SMOOTHNESS).

The parameters used for each of the data reduction techniques are as follows

Blackbody Fit
- Maximum Emissivity (0-1): 1.0
- Lower Wavelength (microns): 7.5
- Upper Wavelength (microns): 8.0

Reference Channel
- Maximum Emissivity (0-1): 1.0
- Reference Wavelength (microns): 7.5

Maximum Spectral Temperature
- Maximum Emissivity (0-1): 1.0
- Instrument Signal-to-Noise: 1000
- Outlier Filtering Factor: 5.0
- Emissivity Tolerance: 0.001
- Lower Wavelength (microns): 8.0
- Upper Wavelength (microns): 14.0

Spectral Smoothness
- Lower Wavelength (microns): 8.12
- Upper Wavelength (microns): 8.6
- Lower Bounding Temperature (K): 280.0
- Upper Bounding Temperature (K): 360.0

Tables 1 through 4 summarize the mean absolute and maximum errors observed between the laboratory spectra measured by the AFRL laboratory and the field spectra collected by SITAC in the longwave portion of the spectrum. Each table represents the results obtained for a particular data reduction / temperature-emissivity separation technique. Figure 1 shows the mean absolute error as a function of technique along with associated 95% confidence intervals. The error statistics computed in the LWIR portion of the spectrum utilize all spectral data between 8 and 14 μm.

Figures 2 and 3 compare the field and laboratory emissivity spectra by data reduction technique for two example materials. The MWIR and LWIR spectra are shown separately to allow more detail to be seen.

As shown in Figures 2 and 3, the field data collected in the midwave portion of the spectra exhibit far less agreement with laboratory measurements than does the equivalent longwave data. Error statistics are not currently shown in this paper for this region since the relevancy of this data is questionable to begin with.

Figure 1 clearly illustrates that the blackbody fit, reference channel, and maximum spectral temperature techniques all produce results that are statistically indistinguishable. The spectral smoothness algorithm, however, does provide results with statistically smaller errors. This, combined with the fact that there are less assumptions and initial guesses that need to be provided by the ground truth collection team, make it the recommended spectral radiance data reduction technique for the LWIR emissivity derivation.

The spectral smoothness algorithm gains its advantage by bringing the spectral emissivity above 13.2 μm more closely in line with the laboratory spectra than the other techniques do. Since this technique works by minimizing the error in derived sample temperature based upon residual atmospheric structure left in the spectrum, it is self-adjusting in a sense and can provide very good results that are not dependent on the user's knowledge of the material being measured. The user does not need to know the emissivity of the target in a particular portion of the spectrum in order to derive the material's spectral emissivity.

## 5. CONCLUSION

The derivation of longwave infrared (LWIR) emissivity spectra from field measured radiance data can be accomplished with an error in absolute magnitude just over 1%. Several methodologies have been implemented and demonstrated in this study, all of which have performed with less than a 2% error in spectral emissivity across the longwave infrared window. The spectral smoothness method, which relies upon the removal of residual atmospheric effects from the derived emissivity spectra, performed the best statistically, with an absolute error across the region of 1.13%. The derivation of midwave infrared (MWIR) emissivity did not perform as well due to numerous factors will be discussed in detail in a second paper appearing in these proceedings by Salvaggio and Miller. These factors include low signal levels, the effects of direct and scattered solar irradiance, and the need for high sample surface temperatures. These factors combine to make measurements in this region of the spectrum an exercise in compromises, none of which yield an optimum result. It is important to note that in this region of the spectrum, one can only expect reasonable results from field measurements in the 4.6 to 5 μm window to the red side of the $CO_2/N_2O$ absorption band under ideal atmospheric and thermodynamic circumstances.

## REFERENCES

1. Hook, S.J. and A.B. Kahle, 1996, The micro Fourier transform interferometer (μFTIR) – A new field spectrometer for acquisition of infrared data of natural surfaces, Remote Sensing of Environment, v. 56, p.172-181.
2. Korb, A.R., P. Dybwad, W. Wadsworth, and J.W. Salisbury, 1996, Portable Fourier transform infrared spectrometer for field measurements of radiance and emissivity, Applied Optics, v. 35, p. 1679-1692.
3. Kahle, A.B. and R.E. Alley, 1992, Separation of temperature and emissivity in remotely sensed radiance measurements, Remote Sensing of Environment, v. 42, p. 107-111.
4. Korb, A.R. and D.M. D'Aria, 2000, Spectral emissivity and temperature retrieval algorithms and software for infrared remote sensing data, Remote Sensing of Environment (in publication).
5. Salisbury, J.W. and D.M. D'Aria, 1992, Emissivity of terrestrial materials in the 8-14 μm atmospheric window, Remote Sensing of Environment, v. 42, p. 83-106.
6. Salisbury, J.W. and D.M. D'Aria, 1994, Emissivity of terrestrial materials in the 3-5 μm atmospheric window, Remote Sensing of Environment, v. 47, p. 345-361.
7. Horton, K.A., J.R. Johnson, and P.G. Lucey, 1998, Infrared measurement of pristine and disturbed soils 2. Environmental effects and field data reduction, Remote Sensing of Environment, v. 64, p. 47-52.
8. Bower, N., R.O. Knuteson, and H.E. Revercomb, High spectral resolution land surface temperature and emissivity measurements in the thermal infrared, Publication from the Co-operative Institute for Meteorological and Satellite Studies at the University of Wisconsin, Madison.

Table 1 Mean absolute and maximum errors between field reduced and laboratory measured LWIR spectral emissivity obtained using the blackbody fit data reduction technique

| | Using BBFIT Technique | | | |
|---|---|---|---|---|
| | Mean Absolute Error | | Maximum Error | |
| Black Silt Screen | 0.0085 | 0.88% | 0.0398 | 4.18% |
| Clear Acetate Film | 0.0218 | 2.28% | 0.0340 | 3.54% |
| Coal | 0.0122 | 1.26% | 0.0179 | 1.84% |
| Commercial Roofing Underlayment | 0.0143 | 1.49% | 0.0329 | 3.45% |
| Foam Core Library Board | 0.0093 | 1.02% | 0.0334 | 4.22% |
| Heavy White Canvas | 0.0138 | 1.53% | 0.0415 | 4.62% |
| Oatley PVC Film | 0.0108 | 1.13% | 0.0400 | 4.19% |
| Particle Board (Fine) | 0.0164 | 1.73% | 0.0416 | 4.37% |
| Polycarbonate Acrylic Sheet | 0.0116 | 1.24% | 0.0386 | 4.14% |
| Silicon Rubber | 0.0099 | 1.05% | 0.0367 | 3.83% |
| White Polyester | 0.0127 | 1.35% | 0.0357 | 3.83% |
| Average | 0.0128 | 1.36% | 0.0356 | 3.84% |
| Standard Deviation | 0.0040 | 0.41% | 0.0070 | 0.79% |

Table 2 Mean absolute and maximum errors between field reduced and laboratory measured LWIR spectral emissivity obtained using the reference channel data reduction technique

| | Using REFCHAN Technique | | | |
|---|---|---|---|---|
| | Mean Absolute Error | | Maximum Error | |
| Black Silt Screen | 0.0090 | 0.93% | 0.0431 | 4.53% |
| Clear Acetate Film | 0.0154 | 1.61% | 0.0282 | 2.95% |
| Coal | 0.0124 | 1.27% | 0.0181 | 1.86% |
| Commercial Roofing Underlayment | 0.0150 | 1.57% | 0.0343 | 3.60% |
| Foam Core Library Board | 0.0143 | 1.53% | 0.0482 | 4.94% |
| Heavy White Canvas | 0.0143 | 1.58% | 0.0422 | 4.70% |
| Oatley PVC Film | 0.0132 | 1.38% | 0.0449 | 4.70% |
| Particle Board (Fine) | 0.0168 | 1.77% | 0.0427 | 4.48% |
| Polycarbonate Acrylic Sheet | 0.0088 | 0.94% | 0.0602 | 6.46% |
| Silicon Rubber | 0.0107 | 1.13% | 0.0414 | 4.32% |
| White Polyester | 0.0224 | 2.46% | 0.0627 | 6.83% |
| Average | 0.0138 | 1.47% | 0.0424 | 4.49% |
| Standard Deviation | 0.0039 | 0.43% | 0.0128 | 1.41% |

Table 3 Mean absolute and maximum errors between field reduced and laboratory measured LWIR spectral emissivity obtained using the maximum spectral temperature data reduction technique

| | Using MAXSPEC Technique | | | |
|---|---|---|---|---|
| | Mean Absolute Error | | Maximum Error | |
| Black Silt Screen | 0.0113 | 1.17% | 0.0539 | 5.66% |
| Clear Acetate Film | 0.0132 | 1.38% | 0.0486 | 5.09% |
| Coal | 0.0171 | 1.75% | 0.0246 | 2.52% |
| Commercial Roofing Underlayment | 0.0188 | 1.97% | 0.0419 | 4.38% |
| Foam Core Library Board | 0.0106 | 1.15% | 0.0315 | 3.98% |
| Heavy White Canvas | 0.0192 | 2.11% | 0.0477 | 5.32% |
| Oatley PVC Film | 0.0124 | 1.30% | 0.0433 | 4.54% |
| Particle Board (Fine) | 0.0187 | 1.97% | 0.0469 | 4.93% |
| Polycarbonate Acrylic Sheet | 0.0084 | 0.90% | 0.0647 | 6.94% |
| Silicon Rubber | 0.0109 | 1.16% | 0.0425 | 4.44% |
| White Polyester | 0.0251 | 2.75% | 0.0726 | 7.91% |
| Average | 0.0151 | 1.60% | 0.0471 | 5.06% |
| Standard Deviation | 0.0051 | 0.56% | 0.0135 | 1.44% |

Table 4 Mean absolute and maximum errors between field reduced and laboratory measured LWIR spectral emissivity obtained using the spectral smoothness data reduction technique

| | Using SMOOTHNESS Technique | | | |
|---|---|---|---|---|
| | Mean Absolute Error | | Maximum Error | |
| Black Silt Screen | 0.0092 | 0.95% | 0.0269 | 2.77% |
| Clear Acetate Film | 0.0242 | 2.53% | 0.0358 | 3.73% |
| Coal | 0.0028 | 0.28% | 0.0094 | 0.96% |
| Commercial Roofing Underlayment | 0.0055 | 0.57% | 0.0157 | 1.64% |
| Foam Core Library Board | 0.0078 | 0.88% | 0.0367 | 4.64% |
| Heavy White Canvas | 0.0235 | 2.57% | 0.0542 | 5.76% |
| Oatley PVC Film | 0.0109 | 1.15% | 0.0248 | 2.58% |
| Particle Board (Fine) | 0.0031 | 0.33% | 0.0115 | 1.22% |
| Polycarbonate Acrylic Sheet | 0.0093 | 1.00% | 0.0556 | 5.96% |
| Silicon Rubber | 0.0083 | 0.89% | 0.0222 | 2.35% |
| White Polyester | 0.0115 | 1.28% | 0.0363 | 4.21% |
| Average | 0.0106 | 1.13% | 0.0299 | 3.26% |
| Standard Deviation | 0.0072 | 0.77% | 0.0156 | 1.74% |

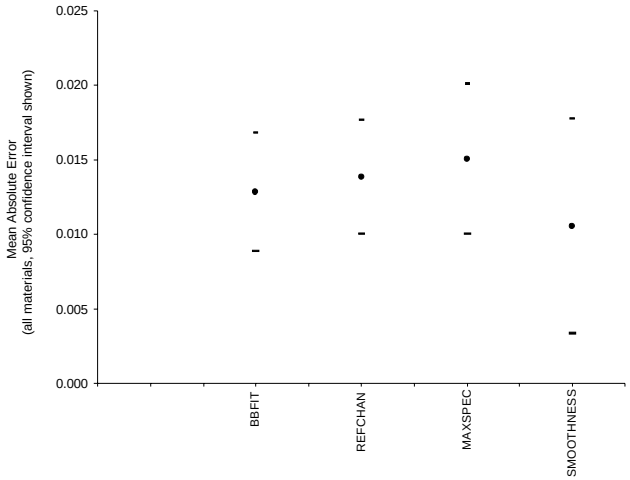


Figure 1 Mean absolute error as a function of data reduction technique for LWIR spectral emissivity

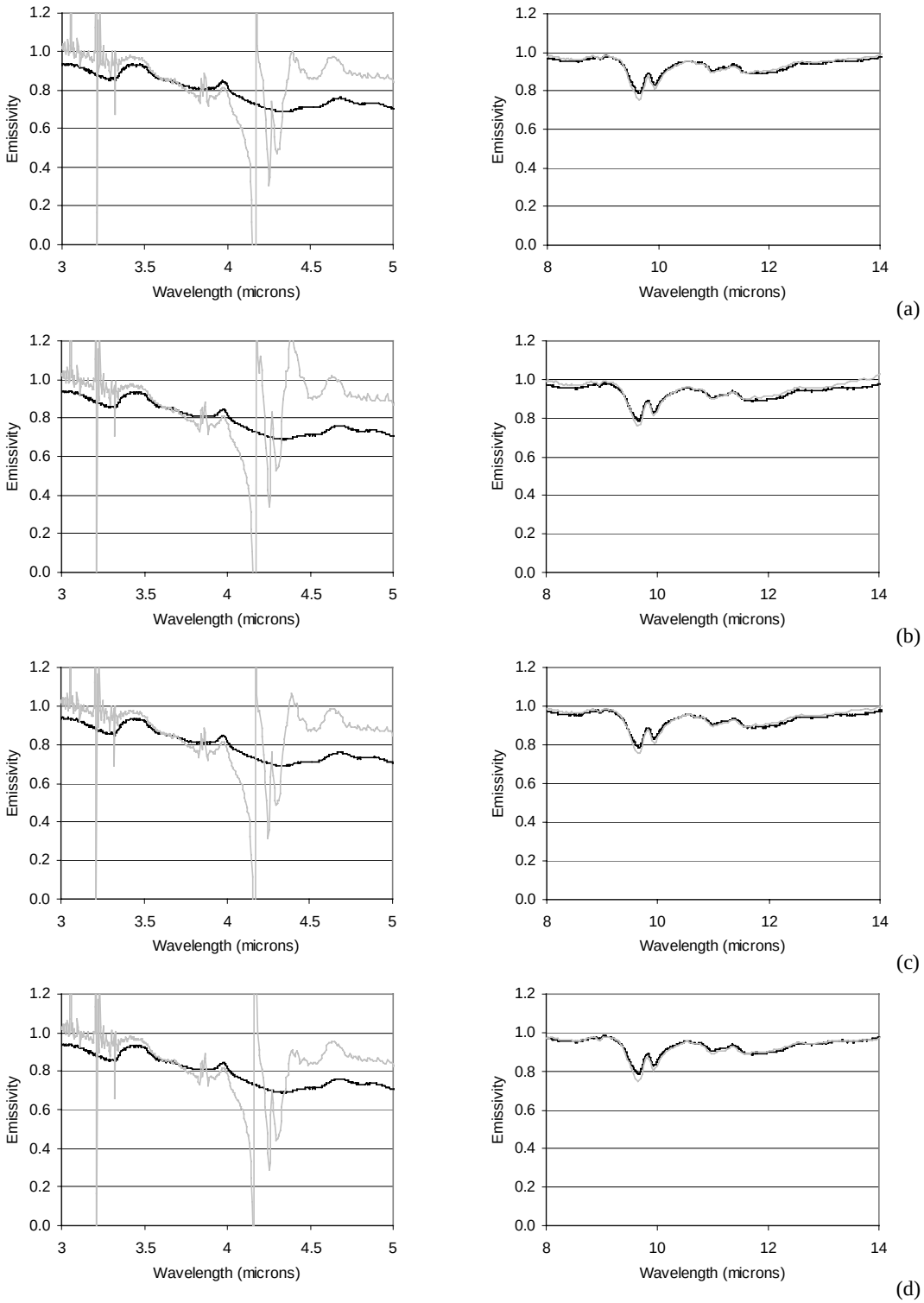


Figure 2 Laboratory measured spectral emissivity (black) for foam core library mount board compared with field measurements (gray) made with SITAC's Designs & Prototypes Model 102 field spectrometer. Four different data reduction/temperature-emissivity separation techniques are shown (a) blackbody fit, (b) reference channel, (c) maximum spectral temperature, and (d) spectral smoothness.

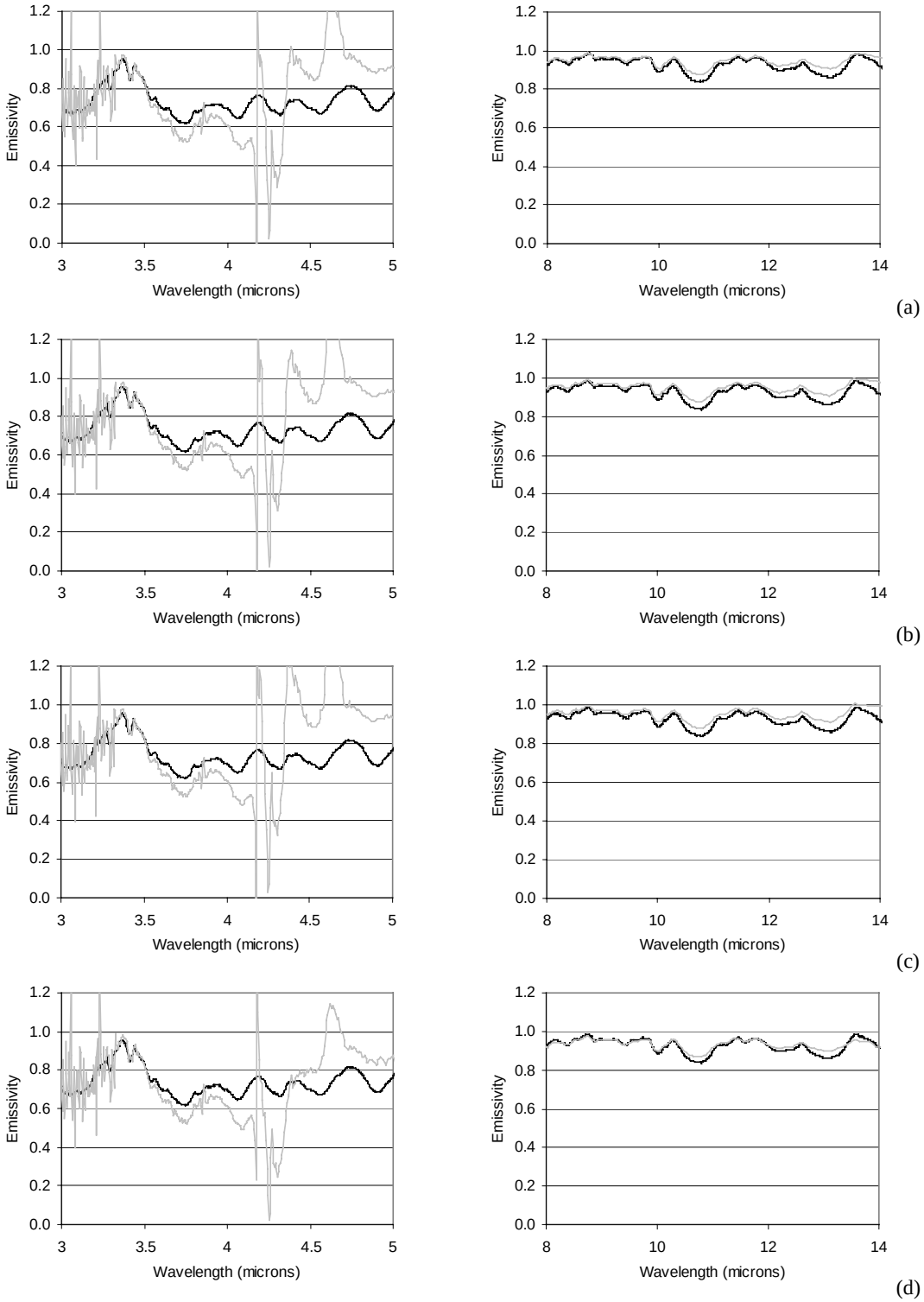


Figure 3 Laboratory measured spectral emissivity (black) for white polyester fabric compared with field measurements (gray) made with SITAC's Designs & Prototypes Model 102 field spectrometer. Four different data reduction/temperature-emissivity separation techniques are shown (a) blackbody fit, (b) reference channel, (c) maximum spectral temperature, and (d) spectral smoothness.